Clim. Past Discuss., 7, 1693–1735, 2011
www.clim-past-discuss.net/7/1693/2011/
doi:10.5194/cpd-7-1693-2011

Climate of the Past Discussions

The oxygen isotopic composition of phytoliths from tropical rainforest soils (Queensland, Australia): application of a new paleoenvironmental tool

A. Alexandre[1], **J. Crespin**[1], **F. Sylvestre**[1], **C. Sonzogni**[1], **and D. W. Hilbert**[2]

[1]CEREGE, UMR6635, CNRS, IRD, Aix-Marseille Université, Europôle de l'Arbois, 13545 Aix en Provence, Cedex 04, France
[2]CSIRO Ecosystem Sciences, Tropical Forest Research Centre, P.O. Box 780, Atherton, QLD 4883, Australia

Received: 21 April 2011 – Accepted: 23 May 2011 – Published: 27 May 2011

Correspondence to: A. Alexandre (alexandre@cerege.fr)

Published by Copernicus Publications on behalf of the European Geosciences Union.

Abstract

Variations in the oxygen isotopic composition of precipitation ($\delta^{18}O_{precipitation}$) in intertropical areas mainly record variations in water sources, amounts of precipitation, and atmospheric temperature and provide information regarding local climate and regional atmospheric circulation changes. On continents, fossil biogenic minerals and speleothems formed in isotopic equilibrium with water can produce continuous $\delta^{18}O$ records and are becoming increasingly valuable for reconstructing past climate changes. Here, we explore the efficiency and limitations of using the oxygen isotopic composition of wood phytoliths ($\delta^{18}O_{wood\ phytolith}$) from tropical rainforest soils as a suitable proxy for atmospheric temperature and $\delta^{18}O_{precipitation}$ values, under conditions that are assumed to be non-evaporative. Soil phytolith assemblages, that should contain 100s of years of phytolith production, were collected along four altitude, temperature, and precipitation gradients in the Queensland rainforests (Australia). Oxygen isotopic analyses were performed on 1.6 mg phytolith samples, after controlled isotopic exchange (CIE), using the IR Laser-Heating Fluorination Technique. Long-term mean annual precipitation (MAP) and mean annual temperature (MAT) values at the sampled sites were obtained using a regional GIS database. The $\delta^{18}O_{precipitation}$ values were estimated. The $\delta^{18}O_{wood\ phytolith}$ values from the leeward slopes were scattered but recorded the modern combination of weighted mean annual $\delta^{18}O_{precipitation}$ values and MAT. The empirical relationship was $\Delta^{18}O_{wood\ phytolith-precipitation}$ (‰ vs. VSMOW) = $-0.4\,(\pm0.2)\ t\ (^{\circ}C) + 46\ (\pm3)$ ($R^2 = 0.4$, $p < 0.05$; $n = 12$). $\delta^{18}O_{precipitation}$ estimates were close to estimates for $\delta^{18}O_{forming\ water}$ when using the temperature-dependant relationships previously described for sedimentary diatoms and natural quartz. However, they were 3‰ higher than estimates for $\delta^{18}O_{forming\ water}$ when using the fractionation relationship obtained for harvested grass phytoliths. The shift may result from estimates uncertainties and/or partial dissolution of soil phytolith assemblages. At this stage, the absence of a uniform temperature-dependant relationship

CPD
7, 1693–1735, 2011

for the different silica-water couples prevents the reconstruction of precise values for $\delta^{18}O_{forming\ water}$ and temperatures from fossil samples. At the same time, the obtained temperature coefficient of −0.4 (±0.2) ‰/°C is in agreement with the fractionation coefficients previously obtained for harvested grass phytoliths, sedimentary and fresh diatoms, and natural quartz. The consistency supports the efficiency of $\delta^{18}O_{wood\ phytolith}$ signatures in recording relative changes in mean annual $\delta^{18}O_{soilwater}$ values (assumed to be equivalent to the weighted mean annual $\delta^{18}O_{precipitation}$ values in rainforest environments) and MAT, provided these changes were on the order of several ‰ and/or several °C in magnitude. While rainforest dynamics can be revealed by morphological phytolith indices, the $\delta^{18}O$ analysis of rainforest phytolith assemblages from continuous sedimentary sequences should simultaneously provide insights into terrestrial climate changes.

1 Introduction

Variations in the oxygen isotopic composition of precipitation ($\delta^{18}O_{precipitation}$) in intertropical areas mainly record variations in water sources, amounts of precipitation, and atmospheric temperature and provide information regarding local climate and regional atmospheric circulation changes (e.g. Dansgaard, 1964; Gat and Matsui, 1991; Rozanski et al., 1993; Fricke and O'Neil, 1999; Gat, 2000; Gat et al., 2001; Poage and Chamberlain, 2001). On continents, fossil biogenic minerals and speleothems formed in isotopic equilibrium with water can produce continuous $\delta^{18}O$ records and are becoming increasingly valuable for reconstructing past climate changes (e.g. von Grafenstein et al., 1999; Genty et al., 2003; Mc Dermott, 2004; Lecuyer et al., 2004; Wang et al., 2005; Leng and Barker, 2006; Liu et al., 2009; Yanes et al., 2010; Dayem et al., 2010). Here, we explore the efficiency and limitations of using the oxygen isotopic composition of wood phytoliths ($\delta^{18}O_{wood\ phytolith}$) from tropical rainforest soils as a suitable proxy for atmospheric temperature and $\delta^{18}O_{precipitation}$ values, under conditions that are assumed to be non-evaporative.

CPD
7, 1693–1735, 2011

Phytoliths are micrometric particles (<60–100 µm of diameter) of amorphous silica that form within a matter of hours to days (Perry et al., 1987) inside or between the cells of higher plant tissues throughout the life of a plant. With plant decay, phytoliths are either incorporated into soils or exported to sediments via regional watersheds. Well preserved in oxidizing environments, phytoliths are recovered from modern to Tertiary materials (e.g. Stromberg et al., 2005). Through the morphological identification of phytolith types, modern and fossil phytolith assemblages have been shown to be a reliable tool for characterizing either the variety of inter-tropical grasslands and for inferring tree cover density at low elevation tropical sites (e.g. Alexandre et al., 1998; Boyd et al., 2005; Bremond et al., 2005a, b, 2008a, b; Piperno, 2006; Lentfer and Torrence, 2007; Neuman et al., 2009).

In parallel with the increasing use of morphological assemblages of phytoliths as vegetation proxies, pioneering studies of the $\delta^{18}O$ signature of phytoliths were conducted using harvested grasses grown under measured conditions of temperature, relative humidity, and isotopic compositions of plant and soil waters (Shahack-Gross et al., 1996; Webb and Longstaffe, 2000, 2002, 2003, 2006). Such studies have demonstrated, in agreement with previous results (e.g. Ometto et al., 2005), that the absorption of water by roots is a non-fractionating process and that in non-transpiring grass stem tissues, the equilibrium fractionation between water and phytolith is temperature-dependent; the temperature coefficient being of −0.33 ‰/°C (recalculated from Shahack-Gross et al., 1996). They additionally evidenced that in transpiring tissues, ^{18}O enrichment of sap water increases with the inverse of relative humidity, which prevents the use of the $\delta^{18}O$ signature of phytoliths from grass leaves as a function of temperature and the isotopic composition of soil water ($\delta^{18}O_{soilwater}$) (Webb and Longstaffe, 2000; 2002; 2006). These calibration studies, although extremely useful for our understanding of the temperature and soil-water $\delta^{18}O$ signals carried by phytoliths, have not lead to paleoenvironmental reconstructions due to the fact that phytoliths from both transpiring and non-transpiring grass tissues are not morphologically distinguishable.

CPD
7, 1693–1735, 2011

In light of these results, we measured the oxygen isotopic composition of rainforests phytolith assemblages collected from the soil humic horizon (or soil top) in the Wet Tropics of North-East Queensland, Australia. We investigated whether a temperature-dependant relationship between the oxygen isotopic composition of wood phytoliths ($\delta^{18}O_{\text{wood phytolith}}$) and $\delta^{18}O_{\text{precipitation}}$ values can be obtained and if it is close to the one previously obtained between isotopic compositions of harvested grass phytolith and plant water.

We focused on Queensland rainforest soil top phytolith assemblages with the overall objectives of paleoenvironmental reconstructions for the following reasons: (1) in small lake's catchments covered by rainforest such as the ones found in Queensland (e.g. Haberle, 2005; Kershaw et al., 2007), phytoliths from eroded soil tops are expected to constitute the main source of fossil phytoliths in sediments; (2) the weak concentration of phytoliths in rainforest soil tops (a few ‰ in weight, Alexandre et al., 1997) and in the suspended load of tropical rivers (less than 5 ‰ in weight, Carry et al., 2005) suggests that the mean phytolith concentration in lake sediments is also on the order of a few ‰ in weight. Taking into account the amount of phytoliths required for $\delta^{18}O$ analyses (several mg) and using the lake sediment accumulation rates commonly observed in Queensland rainforest environments (cm 100 yr^{-1}; e.g. Haberle, 2005; Rieser and Wust, 2010), the fossil phytolith assemblages provided using sampling intervals of several centimeters in lake sediment cores should encompass 100s of years. For comparison, mean age of 100s of years was measured for bulk organic matter (OM) from one of the soil top samples investigated in the present study (^{14}C mean age of sample #18 was 610 ± 15 yr BP; AMS-^{14}C UCIAMS #75077), and can be reasonably expected for phytoliths (Alexandre et al., 1999); direct ^{14}C AMS-measurements of phytolith-occluded carbon, although very promising, being still in a calibration phase (Prior et al., 2005; Rieser et al., 2007; review in Santos et al., 2010); (3) phytolith assemblages from rainforests should carry a $\delta^{18}O$ signature suitable for paleoenvironmental interpretations. Indeed, they are constituted by more than 80 % of a type of phytolith (Alexandre et al., 1997; Runge, 1999; Bremond et al., 2005b), named as Globular granulate after the

CPD
7, 1693–1735, 2011

international code for phytolith nomenclature (Madella et al., 2005), mainly formed in the xylem of the wood of rainforest trees (Scurfield et al., 1974; Kondo et al., 1994) (Fig. 1). Wood is a non-transpiring organ and the isotopic composition of xylem water transported from the roots throughout the plant is not modified by transpiration. Hence, the $\delta^{18}O_{\text{wood phytolith}}$ signature should relate to the $\delta^{18}O_{\text{soil water}}$ signature; (4) the area of the wet tropical rainforests of northeast Queensland, confined to 18 000 km^2, bordered by the Pacific to the east and dry woodlands and savannas to the west, encompasses a large altitude gradient (0–1600 m a.s.l.) with steep gradients in temperature and precipitation (16–25 °C and 1000–8000 mm yr^{-1}) over a short distance (DASETT, 1986). Such gradients are ideal for assessing climatic and altitude controls on the $\delta^{18}O$ signature of rainforest phytolith assemblages.

2 Study area

2.1 Geomorphic features

The Wet Tropical rainforests of Queensland extend from 16°27′ to 17°38′ S and from 145°19 to 145°51 W and have been protected as a world heritage area since 1988. The main distribution of rainforests in northern Queensland straddles three geologic and geomorphic regions that are NW-SE or N-S oriented (Fig. 2a and b): the basaltic tablelands, with an average altitude of 760 m a.s.l. on the west; the alluvial, granitic, and metamorphic lower coastal belt (0–900 m a.s.l.) on the east that includes a coastal plain and a coastal range; and the intermediate granitic and metamorphic eastern highlands with isolated peaks up to 1545 m a.s.l. (Mt. Belleden Ker) and 1622 m a.s.l. (Mt. Bartle Frere). The eastern highlands and the tablelands belong to the Great Dividing Range. Red or yellow loams, red podzolic soils, xanthozems, and krasnozems were developed throughout the weathering of metamorphic rocks, granite, and basalts.

CPD
7, 1693–1735, 2011

2.2 Climate features

The region is located at the southern limit of an area that is influenced by the Australian Summer Monsoon (ASM). The climate pattern is controlled by the position of the Intertropical Convergence zone (ITCZ) and the monsoon circulation. Over 80 % of mean annual precipitation falls during the November–March interval, supplied by NW monsoonal winds during the earlier phase of the ASM, by S-E trade winds during the later phase of the ASM (Godfred-Spenning and Reason, 2002) and by occasional cyclones. In the NW-SE oriented eastern highlands, there is a very pronounced orographic influence with higher precipitation averages centred around the highest peaks and their eastern slopes, windward to the moist prevailing SE airstream. Mean annual precipitation reaches 4000 mm yr^{-1} along the coast, increasing with elevation to reach 11 000 mm yr^{-1} at Mt Bartle Frere, and falls dramatically inland (1200 mm yr^{-1} on the western Tableland) (Fig. 2c). At higher ranges (from 1000 m a.s.l.), fog and orographic cloud layers shroud the summits of the mountains and maintain moist conditions throughout the year. Fog deposition accounts for approximately 40 % of the water reaching the forest floor (Hutley et al., 1997). The amount of water derived from the canopy interception, also called "cloud stripping" by these high-altitude "cloud-forests", can account for 66 % of precipitation during the dry season (McJannet et al., 2007a, b). Coastal humidity averages 78 % in the summer but often reaches values higher than 90 %. Mean annual temperature (MAT) exceeds 24 °C along the coast and falls to below 21 °C on the tableland, and to below 17 °C in the highest ranges (DASETT, 1987; Moss and Kershaw, 2000; Godfred-Spenning and Reason, 2002; Robertson et al., 2005).

2.3 Vegetation features

Rainforests of the wet tropics of Queensland are classified into 27 structural categories that contain more than 3000 plant species from 210 families (Tracey, 1982; Webb and Tracey, 1994). Soils were sampled from areas that support seven rainforest categories

CPD
7, 1693–1735, 2011

(Table 1), numbered and described by Tracey (1982) as follows: Type 16 g (medium and low woodlands) occurs in wet and moist zones on metamorphic foothills. Canopies average 15–20 m. Eucalyptus and Acacia species are common. The ground layer is rich in grasses (e.g. *Imperata cylindrica*). Type 1 (complex mesophyll vine forests) occurs on the highly fertile basaltic and alluvial soils on the tropical humid lowlands. The canopy level reaches 20–40 m. Most of the trees are evergreens. Woody lianes, vascular epiphytes, tree palms, and fleshy herbs with wide leaves (e.g. zingibers and aroids) are prominent. Type 2 (mesophyll vine forests) occurs on granite and schist shallow soils of low to medium fertility, below 400 m a.s.l. The canopy is 30 m high. The forest has a combination of structural features intermediate between those of complex mesophyll and simple notophyll types. Type 5 (complex notophyll vine forests) occur on the tableland, on the wet uplands and highlands, and on the basic volcanic soils. The canopy is 20–45 m high. Robust woody lianes and epiphytes, aroids and zingibers are conspicuous life forms. Dense ground ferns, tree ferns, and palms are present (type 5a). Type 8 (simple notophyll vine forest) occurs between 400 and 1000 m a.s.l. on granitic ranges. Canopy is 23–33 m high. Tree palms are often locally common. Ground ferns are abundant. Canopy is stunted and wind-sheared on exposed ridges, grading into type 9. Type 9 (simple microphyll vine-fern forest) occurs between 800 and 1300 m a.s.l., on granite soils of the cloudy wet highlands. The canopy is 10–25 m high, and the trees are evergreens. Only two or three layers are noticeable. Epiphytes are common. A dense ground layer is characteristic and composed of ferns, palms, and herbs. Forests of this type are also called “cloud” or “wet montane” forests. Type 24 (cleared areas) is made of complex mesophyll vine forest fragments, sugar-cane in the lowlands, and mixed farming in the uplands. Sampling was performed under the forest remnants.

CPD
7, 1693–1735, 2011

3 Materials

Seventeen samples were collected from poorly drained podzolic soils, along four altitudinal transects from 70 to 1283 m a.s.l. (Table 1; Figs. 2 and 3). The sampling method consisted of collecting individual sub-samples of the upper 2 cm of the soil humic horizon (litter excluded), at random intervals, over an area of 5 × 5 m. Sub-samples were mixed together.

Three transects where samples were collected are located in the eastern highlands, east Atherton, while the fourth transect (Northern Cairns) is located on the coastal belt. The "Bartle Frere" transect is located on the North-Western slope of Bartle Frere South Peak (1615 m a.s.l.), above Russell River oriented NW-SE when its upstream section crosses the upper rainforest area. All of the sampled points are leeward relative to the dominant S-E trade winds. The "Palmerston Highway" transect is located in the eastern section of the eastern highlands, above the Johnston River valley (NW-SE). The sites sampled are windward to the dominant S-E trade winds. The "Mt. Edith" transect is located on the southern slope of Mont Edith (1149 m a.s.l.). The sites sampled are windward, but the S-E trades first pass over the Bellenden Ker range (maximum altitude of 1545 m a.s.l., mean altitude of 1100 m a.s.l.) before reaching the tablelands and flowing up to Mt. Edith. The "Northern Cairns" transect is located on the coastal belt. The sampled points are windward (Fig. 3) relative to the dominant S-E trade winds.

Long term climate means at the sampling sites (Table 1) were obtained from regional, digital maps of bioclimatic variables that were created using the ANUCLIM software (McMahon et al., 1995) which uses a Digital Elevation Model (DEM) and meteorological data from a large number of stations over variable time periods (from several to many decades until approximately 2000) to estimate the climate variables for each grid cell in the DEM (0.1 km^2).

CPD
7, 1693–1735, 2011

4 Methods

4.1 Phytolith chemical extraction

Phytoliths were extracted from 20 g of dry soil slightly crushed and sieved at 2 mm, after which the following steps were applied (Kelly, 1999; Crespin et al., 2008): (1) dissolution of carbonates using HCl (1 N); (2) an iron oxide reduction performed with trisodium citrate ($C_6H_5Na_3O_7$) at 88.4 g l^{-1} and 1g of sodium dithionite ($Na_2O_4S_2$, H_2O); (3) the oxidation of organic matter performed using H_2O_2 (30 %) until the reaction subsided; (4) a defloculation using a sodium hexametaphosphate $Na(PO_3)_6$ (5 %) solution buffered at pH 7; (5) a sieving of the samples at 60 µm; (6) a clay removal by sedimentation and centrifugation; (7) a densimetric separation of phytoliths carried out with a zinc bromide heavy liquid ($ZnBr_2$) that had a density of 2.3; and (8) drying for at least 24 h. Steps 2 and 3 were carried out at 50 °C as previously recommended (Crespin et al., 2008).

4.2 Phytolith counting

The recovered fraction was mounted on microscope slides in Canada Balsam, for counting at 600X magnification. More than 200 identifiable phytoliths with a diameter greater than 5 µsm and with a taxonomic significance were counted per sample. Repeated counting gave an error of ±3.5 % (SD). Phytoliths were classified according to the classification of Twiss (1992), and improved and completed using the phytolith shape descriptions of Mulholland (1989), Fredlund and Tieszen (1994), Kondo et al. (1994), Alexandre et al. (1997), Barboni et al. (1999), Runge (1999), and Bremond et al. (2008); and named using the International Code for Phytolith Nomenclature 1.0 (Madella et al., 2005). Phytolith types were categorized as follows: (1) dicotyledon tree and shrub types mainly represented by the Globular granulate type produced by the wood (Scurfield et al.,1974; Kondo et al., 1994); (2) a palm Globular echinate type; (3) grass (poaceae) types comprising Acicular, Elongate echinate, Parallelepipedal and

CPD
7, 1693–1735, 2011

cuneiform bulliform cells, and short cells types; and (4) types without taxonomic significance (unclassified). Abundances of the classified phytolith categories were expressed as a percentage of classified phytoliths, while the abundance of unclassified types was expressed as a percentage of the sum of counted phytoliths (Table 2). Two to 60 µm size particles of quartz, iron oxide and charcoal, as well as larger thin remains of OM, were sometimes recovered and hence counted (Table 2).

4.3 $\delta^{18}O_{silica}$ measurements

Phytoliths are hydrous silica particles that contain exchangeable oxygen mostly in hydroxyl groups (Labeyrie and Juillet, 1982; Perry and Keeling-Tucker, 2000). In order to evaluate the amount of exchangeable oxygen, to fix the isotopic composition, and to calculate the isotopic composition of non-exchangeable oxygen ($\delta^{18}O_{silica}$) a controlled isotopic exchange procedure (CIE) was carried out. Two aliquots of 1.6 mg of the same sample were exchanged with vapor from two waters of a known isotopic composition (Crespin et al., 2008). Oxygen extractions were then performed using the IR Laser-Heating Fluorination Technique as described in Alexandre et al. (2006) and Crespin et al. (2008). Oxygen gas samples were directly sent to and analyzed by a dual-inlet mass spectrometer (ThermoQuest Finnigan Delta Plus). The oxygen isotopic results are expressed in the standard δ-notation relative to V-SMOW. The measured $\delta^{18}O$ values of each sample ($\delta^{18}O_{measured1}$, $\delta^{18}O_{measured2}$) were corrected on a daily basis using a quartz lab standard ($\delta^{18}O_{Boulangé\ 50-100\,\mu m} = 16.36 \pm 0.09$ ‰). One to three aliquots of a phytolith lab standard, MSG 40 (Crespin et al., 2008), were run per measurement session in order to verify the effectiveness of the CIE procedure. Replicate analyses of the samples yielded a reproducibility for $\delta^{18}O_{measured}$ better than ±0.5 ‰, except for one sample (#19) (Table 2). The uncertainty or limit of the 90 % confidence interval associated with the calculation of $\delta^{18}O_{silica}$ using a Monte-Carlo simulation, was ±0.5 ‰ (Crespin et al., 2008). During the calibration period, replicate analyses of the international standard NBS 28 gave an average of 9.6 ± 0.17 ‰ (1σ, $n = 13$).

CPD
7, 1693–1735, 2011

A recent inter-laboratory comparison for oxygen isotopic composition of hydrous biogenic silica has evidenced that, when the CEREGE CIE is performed, a methodological bias occurs leading to abnormally high fractionation between the vapour and the exchanged oxygen ($\Delta_{vapour-Oexchanged}$) (Chapligin et al., 2011). Several tests were conducted to examine possible impacts of water-vapour exchange conditions, the amount of silica subjected to exchange and the rate of silica dehydration. None of these tests produced significant changes in the $\delta_{measured}$ values. Additionally, vapour-silica exchanges were carried out at three temperatures (140 °C, 200 °C and 246 °C). Changes in $\delta_{measured}$ values were the ones expected from the temperature-dependency of the equilibrium fractionation factors. The occurrence of additional fractionation during the vapour-silica exchange and/or silica dehydration thus remained unexplained. For a given sample, the methodological bias was however reproducible. Moreover, differences between $\Delta_{vapour-Oexchanged}$ values obtained at CEREGE for the inter-laboratory comparison samples at 140 and 200 °C and $\Delta_{vapour-Oexchanged}$ values previously obtained for diatoms at the same temperatures (Labeyrie and Juillet, 1982) were measured. Differences were invariant with temperature and did not show any relationship with the measured percentage of exchangeable oxygen ($R^2 = 0.08$) but decreased with increasing $\delta^{18}O_{silica}$ values ($R^2 = 0.9$ after outliers removal). This empirical relationship was used to correct the values of $\Delta_{vapour-Oexchanged}$ as follows (Chapligin et al., 2011):

$$\text{Corrected}\Delta_{vapour-Oexchanged} = \Delta_{vapour-Oexchanged\ \text{from Labeyrie and Juillet,1982}} - 1.3^{*}\delta^{18}O_{silica} + 78 \quad (1)$$

The consistency of this correction was verified using an independent data set previously obtained at CEREGE for fresh water diatoms from Annecy Lake (Crespin et al., 2010). The obtained relationship between $\Delta_{diatoms-lake\ water}$ and temperature of the lake allowed defining a corrected relationship:

$$\text{Corrected}\Delta_{diatoms-lake\ water}(\text{vs.VSMOW}) = -0.28(\pm 0.06)t(°\text{C}) + 35.3(\pm 0.9) \quad (2)$$

with a R^2 of 0.7 and a p-value of 0.002, instead of

$$\Delta_{diatoms-lake\ water}(\text{vs.VSMOW}) = -0.16(\pm 0.09)t(°\text{C}) + 39.25(\pm 1.4). \quad (3)$$

CPD
7, 1693–1735, 2011

In a $\Delta_{\text{diatoms-lake water}}$ vs. t diagram, the obtained corrected fractionation line is shifted towards lower values of $\Delta_{\text{diatoms-lake water}}$, lower but close to fractionation lines previously obtained for fresh water diatoms (e.g. Brandriss et al., 1998; Moschen et al., 2005; Dodd and Sharp, 2010).

4.4 Corrections on $\delta^{18}O_{\text{silica}}$ for obtaining $\delta^{18}O_{\text{wood phytolith}}$

Since some rainforest phytolith assemblages contained a small amount of 2–60 µm particles that were not wood phytoliths, corrections were made to calculate $\delta^{18}O_{\text{wood phytolith}}$ values from $\delta^{18}O_{\text{silica}}$ values.

Correction for the presence of quartz particles: Weight correction was made for the amount of quartz particles (less or equal to 3 % of the counted particles in 7 samples) given the lowest $\delta^{18}O_{\text{quartz}}$ value of 8 ‰ attributed to the detrital quartz of metamorphic origin (e.g. Alexandre et al., 2006), and the respective densities of quartz (2.6) and phytoliths (2.3) (Table 3).

Correction for the presence of grass phytoliths: Phytoliths from the grass understorey may originate from transpiring grass leaves and may have $\delta^{18}O$ values slightly enriched relative to wood phytoliths. Webb and Longstaffe (2002) previously demonstrated for a grass species collected from across the North American prairies that the ^{18}O enrichment of leaf phytoliths relative to stem phytoliths increases with the inverse of relative humidity:

$$\Delta^{18}O_{\text{leaf silica-stem silica}} = 12.5/h - 13. \quad (4)$$

According to (Eq. 4), for the 0.6–1 range of relative humidity calculated by the ANUCLIM software for the sampled sites (Table 1), leaf phytolith ^{18}O enrichment should range from 5 to 0.5 ‰. In the absence of measured data on relative humidity in the under-storey, values from Table 1 were used in (Eq. 4) to correct the obtained $\delta^{18}O_{\text{silica}}$ values for the presence of grass phytoliths. This correction is expected to be maximal. Indeed, in the lower canopy vapour pressure deficit is low (0–0.2 kPa; Hutley et al., 1997) and ^{18}O enrichment of leaf water should be weak, as measured in the

CPD
7, 1693–1735, 2011

Amazonian rainforest (Ometto et al., 2005). Results with and without grass phytoliths corrections, were discussed.

Correction for the presence of palm phytoliths: To our knowledge, $\delta^{18}O_{water}$ signatures in forest palm stems and leaves have never been measured. If ^{18}O enrichment is similar for palm and grass phytoliths, (Eq. 4) should also be used to correct the obtained $\delta^{18}O_{silica}$ values for the presence of palm phytoliths. Results with and without palm phytoliths corrections, were discussed.

No correction for the presence of unclassified phytoliths and charcoal: Unclassified phytoliths were assumed to mainly originate from tree wood and were not corrected for. The occurrence of charcoal particles was not corrected either since charcoal is largely made of carbon and should not contribute to the oxygen yield.

No correction for the presence of organic matter (OM): Thin organic matter remains, most of them with surface ranging from 100 to 200 µm, were counted. They accounted for less or equal to 5 % in 5 samples and for 12 % in one sample (Table 2). No correction was made for their low proportion as they should be oxidized at 1100 °C during CIE sintering step, and removed from the analyzed sample.

4.5 Estimation of atmospheric temperature and $\delta^{18}O_{precipitation}$ values

Ideally, matching the time span recorded by the soil phytolith assemblages would require us to obtain, for each of the sampled sites, measurements for 100s of years for MAT, $\delta^{18}O_{soil\ water}$ and/or $\delta^{18}O_{precipitation}$ values, which is unrealistic. Therefore, estimates were made, as justified below.

Regarding atmospheric temperature, measurements back to 1910 revealed a fast increase of MAT of +0.1 °C/10 y, mostly during the second half of the 19th century in Queensland (Suppiah et al., 2001). To our knowledge there is no other continuous record of temperature from any tropical Australian site. A dendroclimatological study showed evidence of a much slower increasing trend of +1.5 °C since the 16th century in New Zealand (Cook et al., 2000). From these records, the assumption was made that modern long term MAT values extracted from the GIS database (Table 1) should

CPD
7, 1693–1735, 2011

only slightly overestimate (by less than 1–2 °C) the mean value for the last 100s of years; this in a similar way for all the sampled sites.

Regarding precipitation, tree ring reconstruction from the Atherton tableland (Queensland) revealed no long trend since 1861 (Heinrich et al., 2008). In the absence of $\delta^{18}O_{precipitation}$ and/or $\delta^{18}O_{soilwater}$ measurements from Queensland rainforests, assumption was made that the long term depth-weighted $\delta^{18}O_{soilwater}$ values average the long term amount-weight mean annual $\delta^{18}O_{precipitation}$ values. Indeed, because Australian rainforests are characterized by low radiation levels due to frequent occurrence of fog and low clouds and a low range of the vapor pressure deficit for much of the time, soil evaporation and understorey evaporation are expected to be low (Hutley et al., 1997). For comparison, $\delta^{18}O_{soil\ water}$ values measured in the Amazonian rainforest were shown to be close to $\delta^{18}O_{precipitation}$ values and to lie along the local isotopic meteoric water line (Girard et al., 2000). To infer modern $\delta^{18}O_{precipitation}$ values, direct $\delta^{18}O$ measurements could have been performed from non-evaporative surface water (e.g. river, spring water) (Lachniet and Patterson, 2009). However, given the confined sampled area, surface waters did not show sufficient variations in distance from the water source to record rapid changes in $\delta^{18}O_{precipitation}$ values with elevation. Finally, we calculated for each of the sampled site the amount-weighted mean annual $\delta^{18}O_{precipitation}$ value from latitude (LAT), and altitude (ALT) according to the relationships established by Bowen and Wilkinson (2002) from long term data obtained from the International Atomic Energy Agency-World Meteorological Organization Global Network for Isotopes in Precipitation (GNIP) database (IAEA/WMO, 1998). Driving factors, such as the origin of the air masses, the local surface air temperature, the latitude, the "distance from coast", and amount effects (e.g. Dansgaard, 1964; Gat and Matsui, 1991; Rozanski et al., 1993; Fricke and O'Neil, 1999; Gat, 2000; Gat et al., 2001; Poage and Chamberlain, 2001) are implicitly taken into account in these relationships. For stations located <200 m a.s.l. (Eq. 5) and >200 m a.s.l. (Eq. 6) the relationships are respectively expressed as:

CPD
7, 1693–1735, 2011

$$\delta^{18}O_{precipitation} = -0.0051(|LAT|)^2 + 0.1805(|LAT|) - 5.247 \quad (5)$$

$$\delta^{18}O_{precipitation} = -0.0051(|LAT|)^2 + 0.1805(|LAT|) - 0.002(ALT) - 5.247. \quad (6)$$

(Eq. 5) and (Eq. 6) were slightly modified to take regional conditions into consideration: (1) in humid tropics, $\delta^{18}O$ values of precipitation from air masses lifted over high mountains appear to be controlled by the cumulative rainout upwind of collecting stations (Lachniet and Patterson, 2009). The dominance of this rainout process would result, for the windward stations, of an altitude effect of −0.002 ‰/m a.s.l. as measured worldwide (Gonfiantini et al., 2001; Lachniet and Patterson, 2002; Siegenthaler and Oeshger, 1980; Bowen and Wilkinson, 2002; Lachniet and Patterson, 2009), and for the leeward stations, of the delivery of moisture with low $\delta^{18}O$ values (Lachniet and Patterson, 2009), also called "shadow effect"-$\delta^{18}O_{precipitation}$ values are lower than those predicted by altitude effects alone (Rietti-Shati et al., 2000; Longinelli et al., 2006). In order to take into account such a cumulative rainout, especially at leeward sites, the cumulative difference of the altitude crossed by the dominant S-E trade winds before reaching the sampled sites (|ΔALT|) was used for estimating $\delta^{18}O_{precipitation}$ both at the windward and leeward points (Fig. 3; Table 1). The procedure resulted in an inversed isotopic vertical gradient for the leeward slope of Mt. Bartle Frere, neglecting the role of increasing temperature as elevation decreases. This may have led to an underestimate for $\delta^{18}O_{precipitation}$ values especially at leeward low elevation sites; (2) the few isotopic studies investigating the water cycle in Amazonia, Costa-Rica, or Cameroon rainforest areas found an inland ^{18}O gradient of −0.08 ‰/100 km (for areas less than 230 km inland) which reflects the influence of recycled continental moisture (mainly from evapo-transpiration) on the isotopic composition of rain events (Salati et al., 1979; Gat and Matsui, 1991; Martinelli et al., 1996; Njitchoua et al., 1999; Lachniet and Patterson, 2002). Cloud striping that occurs in Queensland rainforests and is not taken into account in the inland gradient should additionally contribute to the rainwash that reaches the soil zone. Water trapped on leaves and undergoing evaporation would contribute to ^{18}O enrichment of soil water and to ^{18}O depletion of the remaining

CPD
7, 1693–1735, 2011

generated vapor that would, in turn, lead to ^{18}O depletion of the following rainfall event, finally increasing the inland ^{18}O gradient. In light of the above considerations, the inland ^{18}O gradient term (−0.08 (DIST)) was added to (Eqs. 5 and 6), keeping in mind that it could be underestimated for cloud forest sites.

Finally, for the <200 m a.s.l. and >200 m a.s.l. sites, the calculation of $\delta^{18}O_{precipitation}$ values was as follows:

$$\delta^{18}O_{precipitation} = -0.0051(|LAT|)^2 + 0.1805(|LAT|) - 5.247 - 0.08(DIST), \quad (7)$$

and

$$\delta^{18}O_{precipitation} = -0.0051(|LAT|)^2 + 0.1805(|LAT|) - 0.002(|\Delta ALT|) - 5.247 - 0.08(DIST). \quad (8)$$

Estimated weighted mean annual $\delta^{18}O_{precipitation}$ values were compared with measured weighted mean seasonal $\delta^{18}O_{precipitation}$ values obtained by CSIRO Land and Water during two rainy seasons in 1998 and 1999, at two stations (Malanda: 17°21′ S; 145°35′ E; 762 m a.s.l. and Walkamin: 17°08′ S; 145°25′ E; 594 m a.s.l.) located in the Atherton tablelands (Fig. 2). We assumed that weighted mean seasonal values were close to the weighted mean annual values, since most of the precipitation occurs during the rainy season. We checked that the $\delta^{18}O$ and δD values measured at Malanda and Walkamine were well aligned along a local meteoric water line with a slope of 8. Measured weighted mean seasonal values for $\delta^{18}O_{precipitation}$ of −8.68 ‰ and −7.77 ‰ were close to the estimated weighted mean annual $\delta^{18}O_{precipitation}$ values of −8.50 ‰ and −7.85 ‰ for Malanda and Walkamine, respectively. The comparison strengthened the reliability of the $\delta^{18}O_{precipitation}$ estimations.

CPD
7, 1693–1735, 2011

5 Results

5.1 Phytolith assemblages

The abundances of tree, palm, grass, and unclassified phytolith categories are presented in Table 2. Four to five phytolith assemblages from the Bartle Frere transect (#35, #36, #37, #38), collected under the cloud forest were dominated by tree wood phytoliths (91 to 100 % of classified phytoliths), while abundances of palm and grass phytoliths ranged from 0–8 % and 0–2 % of classified phytoliths, respectively. Tree, palm, and grass phytoliths accounted for 48 %, 51 %, and 1 %, respectively, of classified phytoliths in the fifth assemblage (#9) that came from the lowest site covered by a rainforest with high floristic richness. Ranges of the abundances of tree, palm, and grass phytoliths in the five assemblages from the Palmerston Highway transect were 76–93 %, 4–19 %, and 1–13 %, respectively, of classified phytoliths. In the four assemblages from the Mt. Edith transect, the abundance of tree, palm, and grass phytoliths were 63–86 %, 8–34 %, and 3–6 %, respectively, of classified phytoliths. The four phytolith assemblages from the Northern Cairns transect showed various abundances of tree, palm, and grass phytoliths: 56–95 %, 0–42 %, and 2–5 % of classified phytoliths, respectively. The phytolith index, D/P (the ratio of ligneous dicotyledons globular granulate (D) over short cell Poaceae phytoliths (P)) was always higher than 12 in agreement with rainforests tree cover density (Bremond et al., 2005b; Bremond et al., 2008a).

Quartz, OM, Fe oxides and charcoal particles were present in low proportions in few samples (Table 2).

5.2 $\delta^{18}O_{silica}$, $\delta^{18}O_{wood\ phytolith}$ and environment

$\delta^{18}O_{measured1}$, $\delta^{18}O_{measured2}$, the percentage of exchangeable oxygen, calculated $\delta^{18}O_{silica}$ values corrected for the CIE methodological bias are presented Table 2. $\delta^{18}O_{wood\ phytolith}$ values corrected for the presence of quartz, grass and palm phytoliths

CPD
7, 1693–1735, 2011

are presented Table 3. Whatever is the non-wood phytolith correction, it is always lower than 0.4 ‰. $\delta^{18}O_{\text{wood phytolith}}$ values, corrected for the presence of quartz only, ranged from 21.2 ‰ to 31.8 ‰ for the assemblages from the Bartle Frere transect, from 33.1 ‰ to 34.6 ‰ for assemblages from Palmerston Highway, from 28.5 ‰ to 31.1 ‰ for assemblages from the Mt. Edith transect, and from 30.8 ‰ to 33.9 ‰ for assemblages from the Northern Cairns transect. The estimated weighted mean annual $^{18}O_{\text{precipitation}}$ values ranged from −8.97 ‰ to −3.67 ‰, for a mean annual temperature range of 17–24.1 °C and a precipitation range of 1500–4942 mm/yr (Table 1). When $\delta^{18}O_{\text{wood phytolith}}$ values (corrected for the presence of quartz) from the leeward transect of Bartle Frere are excluded (Fig. 4) a positive linear correlation with the estimated weighted mean annual $\delta^{18}O_{\text{precipitation}}$ values ($R^2 = 0.55$) occurs, while no trend either with MAT, MAP or elevation appear. Similar patterns are found when $\delta^{18}O_{\text{wood phytolith}}$ values are either additionally corrected for the presence of grass and palm phytoliths (Table 3).

5.3 The relationship between $\delta^{18}O_{\text{wood phytolith}}$ values, $\delta^{18}O_{\text{precipitation}}$ values, and temperature

The $\delta^{18}O$ value of a mineral grown in isotopic equilibrium is a function of the temperature and the oxygen isotopic composition of the water from which it forms ($\delta^{18}O_{\text{forming water}}$), as expressed by

$$[\Delta^{18}O_{\text{mineral-forming water}}] \sim 1000 \ln\alpha = A(10^6/T^2) + B. \quad (9)$$

Over a limited temperature range, the relationship is satisfactorily approximated by a straight line in the plot of $\ln\alpha$ vs. t, expressed as

$$[\Delta^{18}O_{\text{mineral-forming water}}] \sim 1000 \ln\alpha = a\,t + b, \quad (10)$$

given that $\Delta^{18}O_{\text{mineral-forming water}}$ is equal to $\delta^{18}O_{\text{mineral}} - \delta^{18}O_{\text{forming water}}$, α is the fractionation factor, A and a are the fractionation coefficients, B and b are the constants, and T and t are, respectively, the temperature in °K and °C.

CPD
7, 1693–1735, 2011

In the case of rainforest phytoliths, the $\delta^{18}O_{\text{wood phytolith}}$ value should be a function of the atmospheric temperature and, if there is no ^{18}O enrichment between precipitation, soil water, and xylem water, of the $\delta^{18}O_{\text{precipitation}}$value:

$$[\Delta^{18}O_{\text{wood phytolith-precipitation}}] = at + b \quad (11)$$

given that $\Delta^{18}O_{\text{wood phytolith-precipitation}}$ is equivalent to $\delta^{18}O_{\text{wood phytolith}} - \delta^{18}O_{\text{precipitation}}$, $\delta^{18}O_{\text{wood phytolith}}$ is the isotopic composition of wood phytoliths (Table 3), $\delta^{18}O_{\text{precipitation}}$ is the weighted mean annual isotopic composition of precipitation, and t is the MAT (Table 1).

When all $\delta^{18}O_{\text{wood phytolith}}$ values corrected for the presence of quartz are taken into account, no relationship between $[\Delta^{18}O_{\text{wood phytolith-precipitation}}]$ and temperature occurs. When values from the leeward transect of Bartle Frere are excluded a modest correlation (p-value < 0.05) appears (Fig. 5):

$$\Delta^{18}O_{\text{wood phytolith-precipitation}} = -0.4(\pm0.2)t + 46(\pm3), \quad (12)$$

with $R^2 = 0.4$, p-value = 0.037, $n = 12$, or:

$$\Delta^{18}O_{\text{wood phytolith-precipitation}} = 5.2(\pm2)10^6/T^2 - 22(\pm25). \quad (13)$$

When $\delta^{18}O_{\text{silica}}$ values (excepted Bartle Frere values) are corrected for the presence of quartz and grass phytoliths the obtained relationship is close:

$$\Delta^{18}O_{\text{wood phytolith-precipitation}} = -0.4(\pm0.2)t + 47(\pm3), \quad (14)$$

with $R^2 = 0.4$, p-value = 0.027, $n = 12$ or:

When $\delta^{18}O_{\text{wood phytolith}}$ values (excepted Bartle Frere values) are corrected for the presence of quartz, grass and palm phytoliths the obtained relationship changes slightly:

$$\Delta^{18}O_{\text{wood phytolith-precipitation}} = -0.5(\pm0.2)t + 48(\pm4), \quad (15)$$

With $R^2 = 0.35$, p-value = 0.044, $n = 12$.

CPD
7, 1693–1735, 2011

6 Discussion

Whether corrections for the presence of quartz particles, grass and palm phytoliths are made or not on $\delta^{18}O_{silica}$ values, $\Delta^{18}O_{wood\ phytolith-precipitation}$ values obtained for the windward transects showed close negative linear relationships with MAT expressed by their mean temperature coefficients ranging from −0.4 to −0.5 (±0.2) ‰/°C and their y-intercept ranging from 46 to 48 (±4) ‰. These similarities showed the weak influence of the corrections for non-wood phytoliths on $\delta^{18}O$ values of rainforest phytolith assemblages.

6.1 The obtained temperature-dependant relationship: comparison with previous studies

Equation (12) can be compared with the temperature-dependant relationships previously published for different silica-water couples (Fig. 6).

Regarding temperature coefficients, Fig. 6 indicates that the −0.4 (±0.2) ‰/°C value obtained from (Eq. 12) is close to the value obtained for harvested grass phytoliths (−0.33 ‰/°C recalculated from Shahack-Gross et al., 1996) and natural quartz (−0.30 ‰/°C, Sharp and Kirschner, 1994). The coefficient is in the range obtained for fossil diatoms (from −0.28 to −0.49 ‰/°C, Juillet-Leclerc and Labeyrie, 1987; Shemesh et al., 1992), slightly larger than the value experimentally obtained for high temperature quartz (−0.24 to −0.27 ‰/°; Clayton et al., 1972; Matsuhisa et al., 1979), and larger than the value obtained for fresh diatoms (−0.19 to −0.28 ‰/°, Brandriss et al., 1998; Moshen et al., 2005; Dodd and Sharp, 2010; Crespin et al., 2010).

If we focus on the entire temperature-dependant relationships (fractionation lines) Fig. 6 recalls that there is no uniform relationship for the different silica-water couples. Several factors were previously accounted for these discrepancies: diatom frustules that show higher dissolution rate than that of phytoliths (Fraysse et al., 2009) may have been subject to early diagenesis which could have impacted their isotopic composition after deposition (Schmidt et al., 2001; Dodd and Sharp, 2010);

CPD
7, 1693–1735, 2011

approximations of temperature and $\delta^{18}O_{water}$ value may have led to uncertainties on $\Delta^{18}O_{sedimentary\ diatom-water}$ values (Moschen et al., 2005); recrystallization during experimental high temperature quartz-water exchanges may have led to kinetic effects and lowered obtained $\Delta^{18}O_{quartz-water}$ values (Sharp and Kirschner, 1994). Extents of these effects are still to be assessed. In the same time, Fig. 6 indicates that the line obtained from (Eq. 12) is located in between the ones obtained for natural quartz (Sharp and Kirschner, 1994) and sedimentary diatoms (Juillet-Leclerc and Labeyrie, 1987; Shemesh et al., 1992) and the ones obtained for grass phytoliths (Shahack-Gross et al., 1996), fresh water diatoms (Brandriss et al.,1998; Moschen et al., 2005; Dodd and Sharp, 2010; Crespin et al., 2010) and values extrapolated from the high temperature quartz-water fractionation (Clayton et al., 1972; Matshuhisa et al., 1979). For the considered temperature range, our $\delta^{18}O_{precipitation}$ estimates (from Eq. 12) are lower by only 0.2 to 0.9 ‰ than estimates using the fractionation relationship from Juillet-Leclerc and Labeyrie (1987). They are lower by 1.5 to 2.2 ‰ than estimates using the fractionation relationship from Sharp and Kirschner (1994) and higher by 2.5 to 3.2 ‰ than estimates using the fractionation relationship from Shahack-Gross et al. (1996). The relative shift to harvested grass phytoliths may result from the uncertainties associated with the relationships. It can also be explained if calculated $\Delta^{18}O_{wood\ phytolith-precipitation}$ values are higher than actual $\Delta^{18}O_{wood\ phytolith-forming\ water}$ values, due to evaporative ^{18}O enrichment of the soil water absorbed by roots. This may occur if a significant part of the water comes from the first 10s of centimeters of soil during the dry and more evaporative season. However, a greening during the dry season, when it occurs, involves rainforest tree roots' capacity for absorbing non-^{18}O enriched deep soil water rather than shallow water (Huete et al., 2006). Additionally, although biased estimations of $\delta^{18}O_{precipitation}$ and/or discrepancies between $\delta^{18}O_{precipitation}$ and $\delta^{18}O_{soil\ water}$ may have occurred, they should be reproducible in order to explain systematic shifts of several ‰, which is rather unlikely. An underestimation of $\delta^{18}O_{precipitation}$ may also be involved. Although agreement between estimated $\delta^{18}O_{precipitation}$ and measured

CPD
7, 1693–1735, 2011

$\delta^{18}O_{precipitation}$ values on the tablelands (Malanda and Walkamine) support the accuracy of our estimations, obtaining long term $\delta^{18}O_{precipitation}$ and/or $\delta^{18}O_{soilwater}$records (rather than direct measurements only instructive for short term hydrological conditions) for the studied area would help to further verify this accuracy. At least, superficial dissolution of phytoliths in litter and soil (Alexandre et al., 1999) may also lead to slight ^{18}O enrichment as the lighter isotope, forming weaker bonds and having a higher diffusion velocity than the heavier isotope, goes preferentially to the liquid phase. Dissolution figures are difficult to detect on the granulated surface of the Globular granulate phytolith type which prevents verifying the later hypothesis.

6.2 $\delta^{18}O_{wood\ phytolith}$ values obtained from the leeward Bartle Frere transect

Data obtained from Bartle Frere transect did not follow the above relationships, due to particularly low $\Delta^{18}O_{wood\ phytolith-precipitation}$ values drastically decreasing with elevation from samples #35–36 to samples #37–38 (from 39.7 to 31.1 ‰, Table 3, correction for quartz and grass phytoliths) instead of a low temperature gradient (from 17 to 17.9 °C, Table 1). Several points are discussed below to account for this discrepancy: (1) a low temperature gradient may emphasize variations of $\delta^{18}O_{wood\ phytolith}$ values in relation to local environmental changes (e.g. soil evaporation, depth of water uptake, phytolith production), but would unlikely explain a shift as high as 8–9 ‰/°C in $\delta^{18}O_{wood\ phytolith}$ and $\Delta^{18}O_{wood\ phytolith-precipitation}$ values; (2) the four highest sites of the Bartle Frere transect are covered by a cloud forest characterized by cloud striping (Mc Jannete et al., 2007a, b). As previously noted, cloud striping may increase the inland isotopic gradient, enhance the cumulative rainout of ^{18}O depletion in air masses and decrease $\delta^{18}O_{precipitation}$ values. However, cloud forest sites of the windward Mt. Edith transect do not show unexpectedly low $\Delta^{18}O_{wood\ phytolith-precipitation}$ values; (3) the Bartle Frere transect diverges from the three other transects in that it is located leeward relative to the S-E trade winds. Potential $\delta^{18}O_{precipitation}$ underestimation at leeward sites would imply lower $\Delta^{18}O_{wood\ phytolith-precipitation}$ values and cannot account for the discrepancy.

CPD
7, 1693–1735, 2011

N-W monsoonal winds and cyclones with westerly tracks may contribute to precipitation on the N-W slope of Bartle Frere South Peak to a greater extent than on slopes oriented windward. The associated high amount effect (Nott et al., 2007) would decrease the $\delta^{18}O_{precipitation}$ value (and increase associated $\Delta^{18}O_{wood\ phytolith-precipitation}$ values). However, such an effect would likely impact the whole slope and cannot account for decreasing $\Delta^{18}O_{wood\ phytolith-precipitation}$ values with decreasing altitude; (4) the Bartle Frere slope may be subject to higher rain shadow effect than the one taken into account in (Eq. 2), which may lead to overestimate $\delta^{18}O_{precipitation}$ values all the more so altitude decreases. In the literature, the only $\delta^{18}O_{precipitation}$ measured value obtained from a leeward tropical site was about 2‰ lighter than the one expected for a windward site of similar altitude (Gonfiantini et al., 2001).

Finally, without further data, potential combined impacts of canopy interception, storms and rain shadow effects on $\delta^{18}O_{precipitation}$ values are difficult to assess but are rather interesting tracks to investigate in a near future.

6.3 Implications for paleoenvironmental reconstructions

The above comparisons reveal several clues for assessing the efficiency and the limitations for using $\delta^{18}O_{wood\ phytolith}$ values as a proxy for $\delta^{18}O_{precipitation}$ and MAT in rainforest environments.

The absence of a uniform temperature-dependant relationship for different silica-water couples prevents the reconstruction of precise values for $\delta^{18}O_{forming\ water}$ and temperatures from fossil samples. On the other hand, the agreement of the empirical soil phytolith temperature coefficient of −0.4 (±0.2) ‰/°C (Eq. 12) with those previously obtained for different silica-water couples, ranging from 0.2 to 0.5 ‰/C supports its consistency and its reliability for reconstructing, from continuous fossil phytolith sequences, past relative changes in $\delta^{18}O_{soil\ water}$ and $\delta^{18}O_{precipitation}$ values (when both isotopic compositions are assumed to be close) and/or in MAT values. Given its associated ±0.2‰/°C uncertainty it is plausible to expect from the fractionation equation

CPD
7, 1693–1735, 2011

(Eq. 12) reproducible uncertainties of several ‰ and several ˚C on reconstructed changes in $\delta^{18}O_{soil\ water}$ and/or $\delta^{18}O_{precipitation}$ values, and MAT values. Moreover, given the low amount of phytoliths recovered from soils and sediments, we expect the time resolution from sedimendary phytolith records to be limited to hundreds of years. However, such low uncertainty and time resolution are still sufficient for investigating significant terrestrial changes that occurred during the Quarternary glacial/interglacial transitions. If the range of temperature changes can be constrained by other proxies, such as pollen transfer functions, reconstruction of changes in $\delta^{18}O_{soil\ water}$ values using $\delta^{18}O_{wood\ phytolith}$ values should become straightforward. Additionally, the association of morphological and $\delta^{18}O$ analyses on similar tropical forest phytolith assemblages should allow one to assess whether past forest dynamics were or were not synchronous with climate changes. At least a comparison of terrestrial $\delta^{18}O$ records from tropical forest phytolith assemblages with deep-sea reference curves should help to further investigate the relationship between global oceanic transgression/regression phases (e.g. revealed by $\delta^{18}O_{benthic\ foraminifera}$ records) and local changes in the water cycle (revealed by $\delta^{18}O_{phytolith}$ records).

7 Conclusions

Several assumptions were addressed in this study with regard to corrections for non-woody phytoliths and to estimates of precipitation and soil water $\delta^{18}O$ signatures. The related aggregated errors may account for the modest correlation found between $[\Delta^{18}O_{wood\ phytolith-precipitation}]$ and temperature ($R^2 = 0.4$). However, the purpose of this study was not to introduce a new silica-water fractionation curve but, rather to check that an empirical temperature-dependant relationship between $\delta^{18}O_{wood\ phytolith}$ and $\delta^{18}O_{precipitation}$ values could be obtained and was close to fractionation curves previously published for biogenic silica and quartz. The obtained equation (Eq. 12) produced $\delta^{18}O_{precipitation}$ estimates close to $\delta^{18}O_{water}$ estimates using the relationships

CPD
7, 1693–1735, 2011

obtained for sedimentary diatoms (Juillet-Leclerc and Labeyrie, 1987) and natural quartz (Sharp and Kirschner, 1994). However, they were roughly 3‰ higher than estimates for $\delta^{18}O_{\text{forming water}}$ using the temperature-dependant relationship recalculated from Shahack-Gross et al. (1996) for harvested grass phytoliths. The shift may result from the uncertainties associated with both temperature coefficient and y-intercept of the relationships as well as from soil phytolith partial dissolution. At this stage, the absence of a uniform temperature-dependant relationship for different silica-water couples prevents the reconstruction of precise values for $\delta^{18}O_{\text{forming water}}$ and temperature from fossil samples.

At the same time, the temperature coefficient of $-0.4(\pm0.2)$ ‰/°C, obtained from the set of Queensland rainforest soil phytolith assemblages, is close to the fractionation coefficients previously obtained for harvested grass phytoliths, sedimentary diatoms, fresh diatoms and natural quartz. The consistency supports the efficiency of $\delta^{18}O_{\text{wood phytolith}}$ signatures for recording relative changes in mean annual $\delta^{18}O_{\text{soilwater}}$ values (which are assumed to be equivalent to the weighted mean annual $\delta^{18}O_{\text{precipitation}}$ values in rainforests environments) and MAT, provided these changes were several ‰ and/or several °C in magnitude. Morphological phytolith analysis of Quaternary continuous sedimentary sequences from the Western Australo-Pacific area should help to select rainforest phytolith assemblages suitable for $\delta^{18}O$ analysis. The combination of both methods should provide simultaneous insights regarding rainforest dynamics and climate change.

Acknowledgements. This work was conducted during the thesis of J. Crespin PhD (2004–2008) and was partially supported by the Stable Isotope Lab at CEREGE and the French program ECLIPSE. We thank the Sustainable Ecosystems group at the Tropical Forest Research Center (CSIRO) of Atherton who helped us to organize the field trip and who provided the ANUCLIM data. $\delta^{18}O_{\text{precipitation}}$ values measured for Malanda and Walkamine were made available to us by P. G. Cooks and Andrew Herczeg (CSIRO Land and Water). We also thank C. Paillès and C. Vallet-Coulomb (CEREGE) for respectively providing and analyzing the CIE waters, and J. J. Motte (mapping, CEREGE).

CPD
7, 1693–1735, 2011

The publication of this article is financed by CNRS-INSU.

References

Alexandre, A., Meunier, J. D., Colin, F., and Koud, J. M.: Plant impact on the biogeochemical cycle of silicon and related weathering processes, Geochim. Cosmochim. Ac., 61, 677–682, 1997.

Alexandre, A., Meunier, J. D., Lézine, A. M., Vincens, A., and Schwartz, D.: Phytoliths: indicators of grassland dynamics during the Late Holocene in intertropical Africa, Palaeogeog. Palaeoclimatol. Palaeocol., 136, 213–229, 1998.

Alexandre, A., Meunier, J. D., Mariotti, A., and Soubies, F.: Late Holocene paleoenvironmental record from a latosol at Salitre (Southern Central Brazil): phytolith and carbon isotope evidence, Quat. Res., 51, 187–194, 1999.

Alexandre, A., Sonzogni, C., Basile, I., Sylvestre, F., Parron, C., Meunier, J. D., and Colin, F.: Oxygen isotope analyses of fine silica grains using laser-extraction technique: comparison with oxygen isotope data obtained from ion microprobe analyses and application to quartzite and silcrete cement investigation, Geochim. Cosmochim. Ac., 70, 2827–2835, 2006.

Barboni D., Bremond L., and Bonnefille, R.: Comparative study of modern phytolith assemblages from inter-tropical Africa, Palaeogeogr. Palaeoclimatol. Palaeocol., 246, 454–470, 2007.

Bowen G. J. and Wilkinson, B.: Spatial distribution of δ^{18}O in meteoric precipitation, Geology, 30(4), 315–318, 2002.

Boyd, W. E., Lentfer, C. J. and Parr, J.: Interactions between human activity, volcanic eruptions and vegetation during the Holocene at Garua and Numundo, West New Britain, PNG. Quat. Res. 64, 384–398, 2005.

Brandriss, M. E., O'Neil, J. R., Edlund, M. B., and Stoermer, E. F.: Oxygen isotope fractionation between diatomaceous silica and water, Geochim. Cosmochim. Ac., 62, 1119–1125, 1998.

CPD

7, 1693–1735, 2011

Bremond, L., Alexandre, A., Peyron, O., and Guiot, J.: Grass water stress estimated from phytoliths in West Africa, J. Biogeog., 32, 311–32, 2005a.
Bremond, L., Alexandre, A., Hely, C., and Guiot, J.: A phytolith index as a proxy of tree cover density in tropical areas: calibration with Leaf Area Index along a forest-savanna transect in southeastern Cameroon, Global Planet.Change, 45, 277–293, 2005b.
Bremond, L., Alexandre, A., Peyron, O., and Guiot, J.: Grassland biomes estimated from phytoliths in West Africa, J. Biogeogr., 35, 2039–2048, 2008a.
Bremond, L., Alexandre, A., Wooller, M. J., Hély, C., Williamson, D., Schäfer, P. A., Majule, A., and Guiot, J.: Phytolith indices as proxy of grass subfamilies dominance on tropical mountains from three sites in East Africa: Mt Kenya (Kenya), Mt Rungwe and Lake Masoko (Tanzania), Global Planet. Change, 61, 209–224, 2008b.
Canadell, J., Jackson, R. B., Ehleringer, J. R., Mooney, H. A., Sala, O. E., and Schulze, E.-D.: Maximum rooting depth of vegetation types at the global scale, Oecologia, 108, 583–595, 1996.
Cary, L., Alexandre, A., Meunier, J. D., Boeglin, J. L. and Braun, J. J.: Contribution of phytoliths to the suspended load of biogenic silica in the Nyong basin rivers (Cameroon), Biogeochemistry, 74, 101–114, 2005.
Chapligin, B., Leng, M., Webb, E., Alexandre, A., Dodd, J., Faure, K., Ijiri, A., Lücke, A., Shemesh, A., Abelmann, A., Herzschuh, U., Longstaffe, F., Meyer, H., Moschen, R., Okazaki, Y., Rees, N. H., Sharp, Z., Sloane, H. J., Sonzogni, C., Swann, G., Sylvestre, F., Tyler, J., and Yam R.: Interlaboratory comparison of oxygen isotopes from biogenic silica, GCA (manuscript # W8185), submitted, 2011.
Clayton, R. N., O'Neil, J. R., and Mayeda, T. K.: Oxygen isotope exchange between quartz and water, J. Geophys. Res., 77, 3057–3067, 1972.
Crespin, J., Alexandre, A., Sylvestre, F., Sonzogni, C., Paillès, C., and Garreta, V.: IR-laser-extraction technique adapted to oxygen isotopes analysis of small biogenic silica samples, Anal. Chem. 80, 2372–2378, 2008.
Crespin, J., Sylvestre, F., Alexandre, A., Sonzogni, C., Paillès, C., and Perga, M. E.: Re examination of the temperature-dependent relationship between $\delta^{18}O_{diatoms}$ and $\delta^{18}O_{lake\ water}$ for Lake Annecy (France), Implications for palaeoclimatic applications, J. Paleolimnol., doi:10.1007/s10933-010-9436-2, 2010.
Dansgaard, W.: Stable isotopes in precipitation, Tellus 4, 436–468, 1964.
DASETT: Nomination of Wet Tropical Rainforests of North-east Australia by the Government of

CPD
7, 1693–1735, 2011

Australia for inclusion in the World Heritage List. Department of Arts, Sports, the Environment, Tourism and Territories, 31 pp., 1986.
Dayem, K. E., Molnar, P., Battisti, D. S., and Roe, G. H.: Lessons learned from oxygen isotopes in modern precipitation applied to interpretation of speleothem records of paleoclimate from eastern Asia, Earth Planet. Sc. Lett., 295, 219–230, 2010.
Dodd, J. P. and Sharp, Z. D.: A laser fluorination method for oxygen isotope analysis of biogenic silica and a new oxygen isotope calibration of modern diatoms in freshwater environments, Geochim. Cosmochim. Ac., 74(4), 1381–1390, 2010.
Flanagan, L. B., Bain, J. F., and Ehleringer, J. R.: Stable oxygen and hydrogen isotope composition of leaf water in C_3 and C_4 plant species under field conditions, Oecologia, 88, 394–400, 1991.
Fraysse, F., Pokrovsky, O. S., Schott, J., and Meunier, J. D.: Surface chemistry and reactivity of plant phytoliths in aqueous solutions, Chem. Geol., 258, 197–206, 2009.
Fredlund, G. and Tieszen, L. T.: Modern phytolith assemblages from the North American Great Plains, J. Biogeogr., 21(3), 321–335, 1994.
Fricke, H. C. and O'Neil, J. R.: The correlation between $^{18}O/^{16}O$ ratios of meteoric water and surface temperature: its use in investigating terrestrial climate change over geologic time, Earth Planet. Sc. Lett., 170, 181–196, 1999.
Gat, J. R. and Matsui, E.: Atmospheric water balance in the Amazon basin: an isotopic evapotranspiration model, J. Geophys. Res., 96(D7), 13179–13188, 1991.
Gat, J. R.: Atmospheric water balance-the isotopic perspective, Hydrol. Process., 14, 1357–1369, 2000.
Gat, J. R., Mook, W. G. and Meijer, A. J.: Environmental Isotopes in the hydrological cycle. In: Principles and applications IHP-V Technical Documents in Hydrology. 39, UNESCO-IAEA, 2001.
Genty, D., Blamart, D., Ouahdi, R., Gilmour, M., Baker, A., Jouzel, J., and Van-Exter, S.: Precise dating of Dansgaard-Oeschger climate oscillations in western Europe from stalagmite data, Nature, 421, 833–837, 2003.
Girard, J. P., Freyssinet, P., and Chazot, G.: Unraveling climatic changes from intraprofile variation in oxygen and hydrogen isotopic composition of goethite and kaolinite in laterites: an integrated study from Yaou, French Guiana, Geochim. Cosmochim. Ac., 64(3), 409–426, 2000.
Godfred-Spenning, C. R. and Reason, C. J. C.: Interannual variability of lower tropospheric

CPD
7, 1693–1735, 2011

moisture transport during the australian monsoon, Internat. J. Climatol., 22, 509–532, 2002.
Gonfiantini, R., Roche, M. A., Olivry, J. C., Fontes, J. C., and Zuppi G. M.: The alitude effect on the isotopic composition of tropical rains, Chem. Geol., 181, 147–167, 2001.
Haberle, S. G.: A 23,000-yr pollen record from Lake Euramoo, Wet Tropics of NE Queensland, Australia, Quat. Res. 64, 343–356, 2005.
Houlder, D., Hutchinson, M., Nix, H., and McMahon, J.: ANUCLIM User's Guide, Australian National University, Canberra, 2000.
Hsieh, J. C. C., Chadwick, O. A., Kelly, E. F., and Savin S. M.: Oxygen isotopic composition of soil water : quantifying evaporation and transpiration, Geoderma, 82, 269–293, 1998.
Huete, A. R., Didan, K., Shimabukuro, Y. E., Ratana, P., Saleska, S. R., Hutyra, L. R., Yang, W., Nemani, R. R., and Myneni, E.: Amazon rainforests green-up with sunlight in dry season, Geophys. Res. Lett., 33, doi:10.1029/2005GL025583, 2006.
Hutley, L. B., Doley, D., and Yates, D. J.: Water balance of an Australian subtropical rainforest at altitude: the ecological and physiological significance of intercepted cloud and fog, Aust. J. Bot., 45(2), 311–329, 1997.
Jenkinson, D. J. and Rayner ,J. H.: The turnover of soil organic matter in some of the Rothamsted classical experiments, Soil Sci., 123, 298–305, 1977.
Juillet-Leclerc, A. and Labeyrie, L.: Temperature dependence of the oxygen isotopic fractionation between diatom silica and water, Earth Planet. Sc. Lett., 84, 69–74, 1987.
Kelly, E. F.: Methods for extracting opal phytoliths from soils and plant material, Internal Report; Colorado State University, Fort Collins, 1990.
Kershaw, A. P., Bretherton, S. C., and van der Kaars, S.: A complete pollen record of the last 230 ka from Lynch's Crater, north-eastern Australia, Palaeogeog. Palaeoclim. Palaeoecol., 251, 23–45, 2007.
Kondo, R., Childs, C., and Atkinson, I.: Opal phytoliths of New Zealand, Manaaki Whenua Press., p. 85, 1994.
Labeyrie, L. and Juillet, A.: Oxygen isotopic exchangeability of diatom valve silica; interpretation and consequences for paleoclimatic studies, Geochim. Cosmochim. Ac., 46, 967–975, 1982.
Lachniet, M. S. and Patterson, W. P.: Stable isotope values of Costa Rican surface waters, J. Hydrol., 260, 135–150, 2002.
Lachniet, M. S. and Patterson W. P.: Oxygen isotope values of precipitation and surface waters in northern Central America (Belize and Guatemala) are dominated by temperature and

CPD
7, 1693–1735, 2011

amount effects, Earth Planet. Sc. Lett., 284, 435–446, 2009.
Lecuyer, C., Reynard, B., and Martineau, F.: Stable isotope fractionation between mollusc shells and marine waters from Martinique Island, Chem. Geol., 213, 293–305, 2004.
Lentfer, C. and Torrence, R.: Holocene volcanic activity, vegetation succession, and ancient human land use: unraveling the interactions on Garua Island, Papua New Guinea, Rev. Palaeobot. Palynol., 143, 83–105, 2007.
Leng, M. J. and Barker, P. A.: A review of the oxygen isotope composition of lacustrine diatom silica for paleoclimate reconstruction, Earth Sc. Rev., 75(1–4), 5–27, 2006.
Liu, W., Li, X., Zhang, L., An, Z., and Xu, L.: Evaluation of oxygen isotopes in carbonate as an indicator of lake evolution in arid areas: The modern Qinghai Lake, Qinghai-Tibet Plateau, Chem. Geol., 268, 126–136, 2009.
Longinelli, A., Anglesio, E., Flora, O., Iacumin, P., and Selmo, E.: Isotopic composition of precipitation in Northern Italy: Reverse effect of anomalous cliamtic events, J.Hydrol., 329, 471–476, 2006.
Madella, M., Alexandre, A., Ball, T., ICPN Working Group: International Code for Phytolith Nomenclature 1.0, Ann. Bot.-London, 96(2), 253–260, 2005.
Martinelli, L. A., Victoria, R. L., Sternberg, L. S. L., Ribeiro, A., and Moreira, M. Z.: Using stable isotopes to determine sources of evaporated water to the atmosphere in the Amazon Basin, J.Hydrol., 183, 191–204, 1996.
Matsuhisa, Y., Goldsmith, J. R., and Clayton, R. N.: Oxygen isotopic fractionation in the system quartz-albite-anorthite-water, Geochim. Cosmochim. Ac., 43, 1131–1140, 1979.
McMahon, J. P., Hutchinson, M. F., Nix, H. A. and Ord, K. D.: ANUCLIM user's guide, version 1., Centre for Resource and Environmental Studies, Australian National University, Canberra, 1995.
Mc Jannet, D., Wallace, J., and Reddell, P.: Precipitation interception in Australian tropical rainforests: I. Measurment of stemflow, throughfall and cloud interception, Hydrolog. Process., 21, 1692–1702, 2007a.
Mc Jannet, D., Wallace J., and Reddell, P.: Precipitation interception in Australian tropical rainforests: I. Altitudinal gradient of cloud interception, stemflow, throughfall and interception, Hydrolo. Process., 21, 1703–1718, 2007b.
Moschen, R., Lücke A., and Schleser, G. H.: Sensitivity of biogenic silica oxygen isotopes to changes in surface water temperature and paleoclimatology, Geophys. Res. Lett., 32, L07708, doi:10.1029/2004GL022167, 2005.

CPD
7, 1693–1735, 2011

Moss, P. T. and Kershaw, A. P.: The last glacial cycle from the humid tropics of northeastern Australia: comparison of a terrestrial and a marine record, Palaeogeogr. Palaeoclimatol. Palaeoecol., 155, 155–176, 2000.
Mulholland, S. C.: Phytoliths shape frequencies in North Dakota grasses: A comparison to general patterns, J. Archaeol. Sci., 16, 489–511, 1989.
Neumann, K., Fahmy, A., Lespez, L., Ballouche, A., and Huysecom, E.: The Early Holocene palaeoenvironment of Ounjougou (Mali): phytoliths in a miltiproxy context, Palaeogeogr. Palaeoclimatol. Palaeoecol., 276, 87–106, 2009.
Nott, J., Haig, J., Neil, H., and Gillieson, D.: Greater frequency variability of land falling tropical cyclones at centennial compared to seasonal and decadal scales, Earth Planet. Sc. Lett., 255, 367–372, 2007.
Njitchoua, R., Sigha-Nkamdjou, L., Dever, L., Marlin, C., Sighomnou, D., and Nia, P.: Variations of the stable isotopic composition of rainfall events from the Cameroon rainforest, Central Africa, J. Hydrol., 223, 17–23, 1999.
Ometto, J. P. H., Flanagan, L. B., Martinelli, L. A., and Ehrleringer, J. R.: Oxygen isotope ratios of waters and respired CO_2 in Amazonian forest and pasture ecosystems, Ecol. Appl., 15(1), 58–70, 2005.
Parton, W. J., Schimel, D. S., Cole, C. V., and Ojima, D. S.: Analysis of factors controlling soil organic matter levels in Great Plains grasslands, Soil Sci. Sot. Amer. J., 51, 1173–1179, 1987.
Perry, C. C. and Keeling-Tucker, T.: Biosilicification: the role of organic matrix in structure control, J. Biol. Inorg. Chem., 5, 537–550, 2000.
Piperno, D. R. and Becker, P.: Vegetational history of a site in the central Amazon Basin derived from phytolith and charcoal records from natural soils, Quat. Res., 45, 202–209, 1996.
Piperno, D. R.: Phytoliths: a comprehensive guide for archaeologists and paleoecologists, Lanham: Altamira Press, p. 238, 2006.
Poage, M. A. and Chamberlain, C. P.: Empirical relationships between elevation and the stable isotope composition of precipitation and surface waters : considerations for studies of paleoelevation change, Am. J. Sci., 301, 1–15, 2001.
Prior, C. A., Carter, J. A., and Rieser, U.: Are phytolith radiocarbon dates reliable? 10th International Conference on Accelerator Mass Spectrometry, Berkeley, USA (abstr), 2005.
Rieser, U., Carter, J. A., and Prior, C. A.: Phytoliths: a chronometer for the late Quaternary. INQUA 2007 Conference, Cairns, Australia (abstr), 2007.

CPD
7, 1693–1735, 2011

Rieser, U. and Wust, R. A. J.: OSL chronology of Lynch's Crater, the longest terrestrial record in NE-Australia, Quat. Geochronol., 5, 233–236, 2010.
Rietti-Shatti, M., Yam, R., Karlen, W. and Shemesh, A.: Stable isotope composition of tropical high-altitude fresh-waters on Mt Kenya, Equatorial East Africa, Chem. Geol., 166, 341–350, 2000.
Robertson, A. W., Kirshner, S., Smyth, P., Charles, S. P., and Bates, B. C.: Subseasonal-to-Interdecadal variability of the Australian monsoon over North Queensland, Q. J. R. Meteorol. Soc., 131, 1–26, 2005.
Rozanski, K., Araguas-Araguas, L., and Gonfiantini, R.: Isotopic patterns in modern global precipitations, in: Climate change in continental climate records, edited by: Swart, P. K., Lohmann, K. C., Mc Kenzie, J., Savin, S., American Geophysical Union, Geophys. Monogr. 78, 1–36, 1993.
Runge, F.: The opal phytolith inventory of soils in central Africa-quantities, shapes, classification, and spectra, Rev. Palaeobot. Palynol., 107(1–2), 23–53, 1999.
Salati, E., Dall'Ollio, A., Gat, J., and Matsui, E.: Recycling of water in the Amazon basin: an isotope study, Water Resour. Res., 15, 1250–1258, 1979.
Santos, G. M., Southon, J. R., Druffel-Rodriguez, K. C., Griffin, S., and Mazon, M.: Magnesium perchlorate as an alternative water trap in AMS graphite sample preparation: A report on sample preparation at KCCAMS at the University of California, Irvine, Radiocarbon, 46, 165–173, 2004.
Santos, G. M., Alexandre, A., Coe, H. H. G., Reyerson, P. E., Southon, J. R., and De Carvalho, C. N.: The Phytolith ^{14}C puzzle: a tale of background determinations and accuracy tests, Radicarbon, 52–1, 113–128, 2010.
Scurfield, G., Anderson, C. A., and Segnit, E. R.: Silica in woody stems, Austr. J. Bot., 22, 211–229, 1974.
Shahack-Gross, R., Shemesh, A., Yakir, D., and Weiner, S.: Oxygen isotopic composition of opaline phytoliths : potential for terrestrial climatic reconstruction, Geochim. Cosmochim. Ac., 60, 3949–3953, 1996.
Sharp, Z. D. and Kirschner, D. L.: Quartz-calcite oxygen isotope thermometry: A calibration based on natural isotopic variations, Geochim. Cosmochim. Ac., 58, 4491–4501, 1994.
Shemesh, A., Charles, C. D., and Fairbanks, R. G.: Oxygen isotopes in Biogenic Silica: Global Changes in Ocean Temperature and Isotopic Composition, Science, 256, 1434–1436, 1992.
Siegenthaler, U. and Oeschger, H.: Correlation of ^{18}O in precipitation with temperature and

CPD
7, 1693–1735, 2011

altitude, Nature, 285, 314–317, 1980.
Strömberg, C. A. E.: Decoupled taxonomic radiation and ecological expansion of open-habitat grasses in the Cenozoic of North America, PNAS 102(34), 11980–11984, 2005.
Tracey, J. G.: The vegetation of the humid tropical region of North Queensland, CSIRO, p. 128, 1982.
Twiss, P. C.: Predicted world distribution of C3 and C4 grass phytoliths, in: Phytolith Systematiccs. Emerging Issues, edited by: Rapp, G. and Mulholand S. C., Adv. Archeol. Mus. Sci. I, 113–128, 1992.
Von Grafenstein, U., Erlenkeuser, H., Brauer, A., Jouzel, J., and Johnsen, S. J.: A Mid-European decadal isotope-climate record from 15,500 to 5000 years B.P. Science, 284, 1654–1657, 1999.
Wang, Y., Cheng, H., Edwards, R. L., He, Y., Kong, X., An, Z., Wu, J., Kelly, M. J., Dykoski, C. A., and Li X.: The Holocene Asian Monsoon: Links to Solar Changes and North Atlantic Climate, Science, 308, 854–857, 2005.
Webb, J. A. and Golding, S. D.: Geochemical mass-balance and oxygen-isotope constraints on silcrete formation and its paleoclimatic implications in southern Australia, J. Sediment. Res., 68(5), 981–993, 1998.
Webb, L. J. and Tracey, J. G.: The rainforests of northern Australia. In: Australian vegetation., edited by: Groves, R. H., Cambridge University Press, 87–130, 1994.
Webb, E. A. and Longstaffe, F. J.: The oxygen isotopic compositions of silica phytoliths and plant water in grasses: implications for the study of paleoclimate, Geochim. Cosmochim. Ac., 64, 767–780, 2000.
Webb, E. A. and Longstaffe, F. J.: Climatic influences on the oxygen isotopic composition of biogenic silica in prairie grass, Geochim. Cosmochim. Ac., 66, 1891–1904, 2002.
Webb, E. A. and Longstaffe, F. J.: The relationship between phytolith-and plant water $\delta^{18}O$ values in grasses, Geochim. Cosmochim. Ac., 67(8), 1437–1449, 2003.
Webb, E. A. Longstaffe, F. J.: Identifying the $\delta^{18}O$ signature of precipitation in grass cellulose and phytoliths: Refining the paleoclimate model, Geochim. Cosmochim. Ac., 70, 2417–2426, 2006.
Yanes, Y., Romanek, C. S., Delgado, A., Brant, H. A., Noakes, J. E., Alonso, M. R., and Ibanez, M.: Oxygen and carbon stable isotopes of modern land snail shells as environmental indicators from a low-latitude oceanic island, Geochim. Cosmochim. Ac., 73, 4077–4099, 2009.

CPD
7, 1693–1735, 2011

Table 1. Location of the sampled sites and associated climate parameters (D. coast: distance from the coast; Alt: altitude; Max Alt: mean maximum altitude crossed by air masses; MAT: mean annual temperature; MAP: mean annual precipitation; H: relative humidity provided by the ANUCLIM software; rainforest types from Tracey, 1982). $\delta^{18}O_{precipitation}$ values are estimated from (Eq. 7) and (Eq. 8) slightly modified after Bowen and Wilkinson (2002).

Sample #	Transect	Latitude S DMS	Latitude S DD	Longitude E DMS	D. coast m	Alt (m a.s.l.)	Mean Max Alt (m a.s.l.)	MAT (°C)	MAP (mm)	H (%)	Rainforest type	$\delta^{18}O_{precipitation}$ (‰vs. V-SMOW)
9	Bartle frere	17°16′57.1″	17.28	145°37′09.7″	70	770	1600	19.8	1832	82	1	−8.97
38	Bartle frere	17°22′47.7″	17.38	145°47′21.7″	40	1113	1600	17.9	4082	100	8/9	−7.86
37	Bartle frere	17°22′52.1″	17.38	145°47′34.8″	40	1184	1600	17.6	4411	100	8/9	−7.72
36	Bartle frere	17°22′54.2″	17.38	145°47′40.0″	40	1222	1600	17.4	4603	100	8/9	−7.64
35	Bartle frere	17°22′56.5″	17.38	145°47′43.0″	40	1283	1600	17	4942	100	8/9	−7.52
21	Palmerston	17°34′17.4″	17.57	145°49′46.2″	30	190	190	22.7	3333	92	24	−3.67
24	Palmerston	17°36′28.7″	17.61	145°46′17″6	30	405	405	21.7	3154	94	1/2	−4.48
19	Palmerston	17°35′20.1″	17.59	145°36′58.0″	40	810	810	19.6	2516	92	5a	−5.30
18	Palmerston	17°32′04.0″	17.53	145°34′46.9″	40	950	950	19	2281	91	5a	−5.58
17	Palmerston	17°31′13.4″	17.52	145°33′59.8″	40	1050	1050	18.2	2583	95	24	−5.78
16	Mt Edith	17°07′44.8″	17.13	145°37′33.9″	70	670	1500	20.4	1569	72	1	−8.01
15	Mt Edith	17°06′33.5″	17.11	145°37′15.1″	70	750	1500	20	1700	78	8/9	−8.17
14	Mt Edith	17°06′22.3″	17.11	145°36′57.4″	70	840	1500	19.5	1941	82	8/9	−8.35
11	Mt Edith	17°05′35.0″	17.09	145°37′29.2″	70	1150	1500	18	3083	96	8/9	−8.97
28	N Cairns	16°28′20.8″	16.47	145°19′52.8″	30	70	70	24.1	2040	67	1/2	−3.68
29	N Cairns	16°31′21.4″	16.52	145°23′35.1″	30	210	210	23.2	1758	65	16g	−4.10
33	N Cairns	16°48′33.7″	16.81	145°29′36.7″	30	600	600	22.1	1500	71	1b	−4.88

CPD
7, 1693–1735, 2011

Table 2. Phytolith assemblages, non phytolith remains and associated measured and calculated isotopic values.

		Phytolith types and origin				Non phytolith remains				Isotopic measurements						Isotopic calculations[f]				
		Uncl.	Globular (Trees) granulate	Globular (Palms) echinate	Poaceae types[a]	Quartz	OM[b]	Fe Oxides	Charcoal	$\delta^{18}O_{measured1}$ Average	$\delta^{18}O_{measured1}$ SD[c]	$\delta^{18}O_{measured1}$ n[d]	$\delta^{18}O_{measured2}$ Average	$\delta^{18}O_{measured2}$ SD[3]	$\delta^{18}O_{measured2}$ n[d]	X[e]	Precision[f]	$\delta^{18}O_{silica}$	Precision[f]	Corrected[g] $\delta^{18}O_{silica}$
Samples #	Transect	(% sum)	(% classified phytoliths)			(% counted particles)				(‰ vs. VSMOW)			(‰ vs. VSMOW)			(%)		(‰ vs. VSMOW)		(‰ vs. VSMOW)
9	Bartle Frere	15	48	51	1	1	0	1	0	31.23	0.26	3	35.94	0.11	3	9.7	1.4	35.1	0.5	31.6
38	Bartle Frere	4	91	8	1	3	5	0	0	23.50	0.08	2	33.23	0.27	2	20.1	1.4	30.5	0.5	20.8
37	Bartle Frere	9	100	0	0	0	12	0	0	27.28	0.39	2	33.38	0.05	2	12.6	1.4	31.8	0.5	26.6
36	Bartle Frere	19	99	0	1	0	0	0	0	31.06	0.28	3	34.62	0.13	2	7.3	1.4	33.9	0.5	31.2
35	Bartle Frere	13	96	2	2	0	3	0	0	30.23	0.03	2	33.67	0.45	4	7.1	1.4	32.9	0.5	30.2
21	Palmerston	39	76	14	10	0	1	0	0	32.43	0.27	3	37.42	0.16	2	10.3	1.4	36.6	0.5	33.2
24	Palmerston	10	80	19	1	0	0	0	1	33.53		1	36.69	0.17	2	6.5	1.4	36.2	0.5	34.0
19	Palmerston	20	85	6	9	0	1	0	9	31.58	0.68	2	36.17	0.13	2	9.5	1.4	35.3	0.5	32.0
18	Palmerston	24	93	5	2	0	0	0	1	32.74		1	36.15	0.08	2	7.0	1.4	35.5	0.5	33.1
17	Palmerston	37	83	4	13	1	0	3	1	33.79	0.44	3	37.22	0.36	4	7.1	1.4	36.7	0.5	34.4
16	Mt Edith	16	63	34	3	2	0	0	0	30.73	0.29	3	32.97	0.01	2	4.6	1.4	32.4	0.5	30.7
15	Mt Edith	11	70	28	2	0	0	0	3	29.80	0.36	2	33.95	0.08	3	8.6	1.4	33.0	0.5	29.7
14	Mt Edith	31	77	18	5	1	0	0	0	30.50	0.13	3	35.16	0.05	2	9.6	1.4	34.2	0.5	30.6
11	Mt Edith	18	86	8	6	0	0	0	0	28.80	0.12	2	33.85	0.22	2	10.4	1.4	32.6	0.5	28.5
28	N Cairns	18	89	9	2	1	0	0	0	32.04	0.39	3	34.79	0.16	2	5.7	1.4	34.2	0.5	32.2
29	N Cairns	26	95	0	5	2	0	0	0	33.20	0.50	3	35.25	0.08	2	4.2	1.4	34.9	0.5	33.4
33	N Cairns	15	56	42	2	0	2	0	0	30.66	0.24	2	34.89	0.11	2	8.7	1.4	34.0	0.5	30.8

[a] Include acicular, elongate echinate, bulliform cells and short cells.
[b] Organic matter.
[c] Standard deviation. [d] Number of analyses.
[e] Percentage of exchangeable oxygen.
[f] Calculated after Crespin et al. (2008).
[g] Corrected for the amount of non phytolith remain (cf. text).

CPD
7, 1693–1735, 2011

Table 3. $\delta^{18}O_{wood\ phytolith}$ values obtained after correction for the presence of non-wood phytolith types (Table 2) and associated $\Delta^{18}O_{wood\ phytolith-precipitation}$ values.

Samples #	Transect	Corrected $\delta^{18}O_{phytolith}$			$\Delta^{18}O_{wood\ phytolith-precipitation}$		
		a	b	c	a	b	c
		(‰ vs. VSMOW)			(‰ vs. VSMOW)		
9	Bartle Frere	31.8	31.8	31.2	40.8	42.7	40.2
38	Bartle Frere	21.2	21.2	21.3	29.1	31.1	29.1
37	Bartle Frere	26.6	26.6	26.6	34.3	36.3	34.3
36	Bartle Frere	31.2	31.2	31.2	38.8	40.8	38.8
35	Bartle Frere	30.2	30.2	30.2	37.7	39.7	37.7
21	Palmerston	33.2	33.1	33.0	36.8	36.8	36.7
24	Palmerston	34.0	34.0	33.9	38.5	38.5	38.4
19	Palmerston	32.0	31.9	31.9	37.3	37.2	37.2
18	Palmerston	33.1	33.1	33.1	38.7	38.7	38.7
17	Palmerston	34.6	34.6	34.6	40.4	40.4	40.4
16	Mt Edith	31.1	31.0	29.5	39.1	39.0	37.5
15	Mt Edith	29.7	29.6	28.8	37.9	37.8	37.0
14	Mt Edith	30.8	30.7	30.3	39.2	39.1	38.7
11	Mt Edith	28.5	28.5	28.5	37.5	37.5	37.5
28	N Cairns	32.4	32.3	31.8	36.1	36.0	35.5
29	N Cairns	33.9	33.6	33.6	38.0	37.7	37.7
33	N Cairns	30.8	30.7	28.7	35.6	35.6	33.6

a Correction for the presence of quartz particles.
b Correction for the presence of quartz particles and grass phytoliths.
c Correction for the presence of quartz particles, grass and palm phytoliths.

CPD
7, 1693–1735, 2011

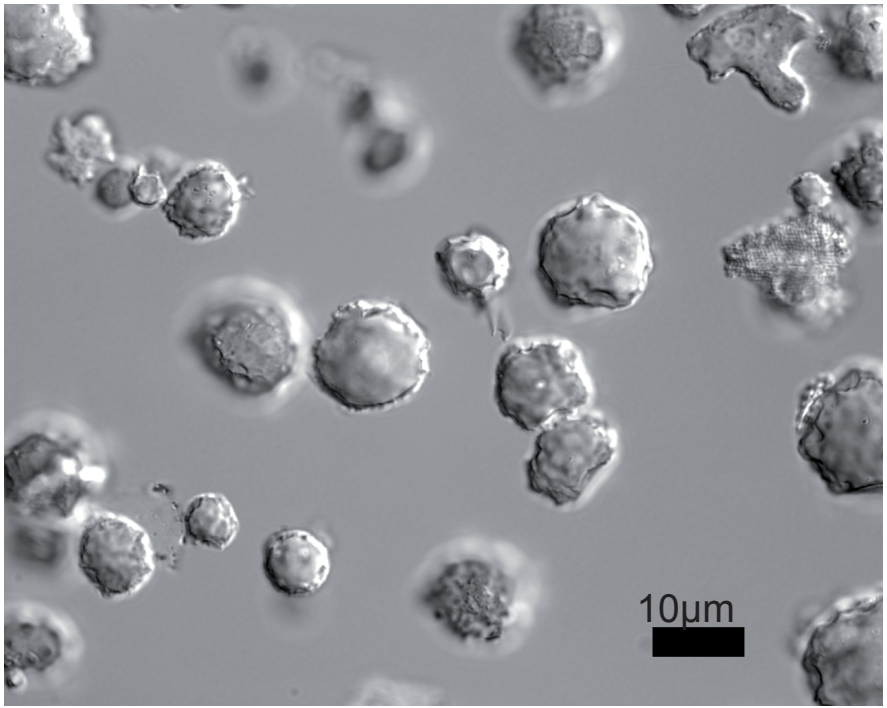

Fig. 1. Phytolith assemblage typical of rainforest, dominated by the "Globular granulate" phytolith type.

CPD
7, 1693–1735, 2011

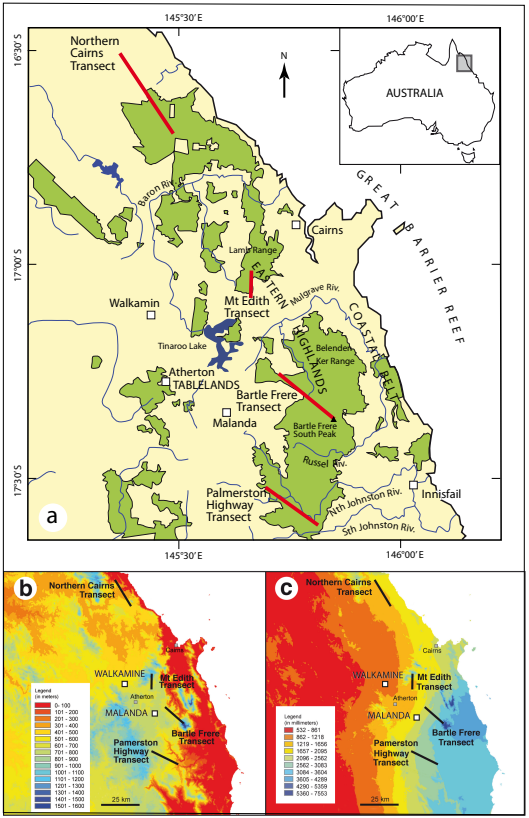

Fig. 2. (a) Location of the rainforests area (in green) in the Wet Tropics of Queensland. **(b)** Altitude and **(c)** mean annual precipitation (MAP) maps generated by the ANUCLIM software (McMahon et al., 1995). Sampled transects and stations of Malanda and Walkamine for which measured $\delta^{18}O_{precipitation}$ data is available are positioned.

CPD
7, 1693–1735, 2011

The oxygen isotopic composition of phytoliths from tropical

A. Alexandre et al.

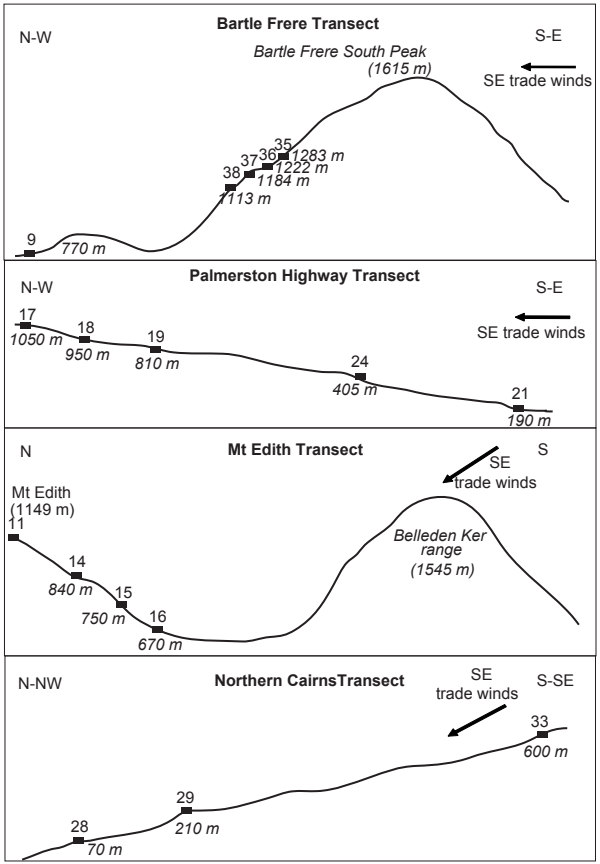

Fig. 3. The four sampled transects: topography and location relatively to the dominant S-E trade winds. Numbers refer to the sampled sites. Altitude is indicated in m a.s.l. (Table 1).

CPD
7, 1693–1735, 2011

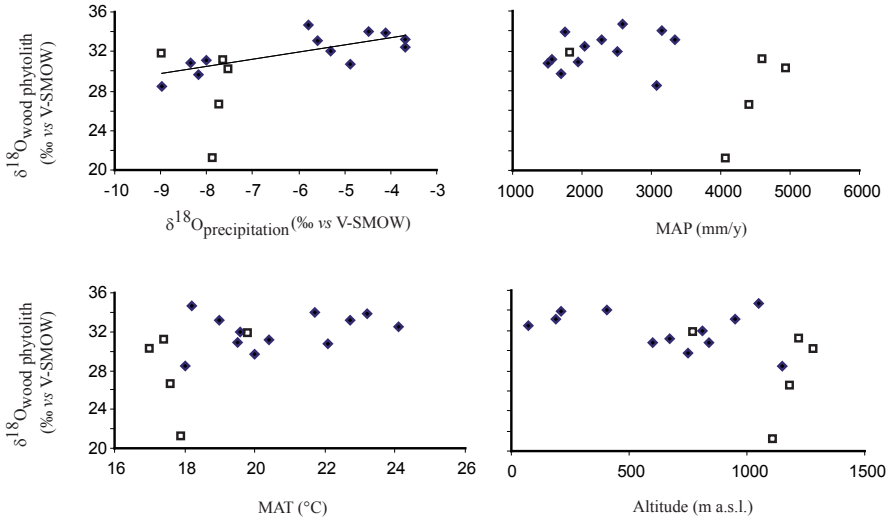

Fig. 4. $\delta^{18}O_{\text{wood phytolith}}$ values (corrected for the presence of quartz) vs. altitude, mean annual temperature (MAT), mean annual precipitation (MAP) and estimated amount weighted mean annual $\delta^{18}O_{\text{precipitation}}$ values. Precision on $\delta^{18}O_{\text{wood phytolith}}$is ±0.5 ‰. A linear positive correlation appears between $\delta^{18}O_{\text{wood phytolith}}$ and $\delta^{18}O_{\text{precipitation}}$ values ($R^2 = 0.5$). Points from Bartle Frere transect (empty squares) are excluded from the correlation.

CPD
7, 1693–1735, 2011

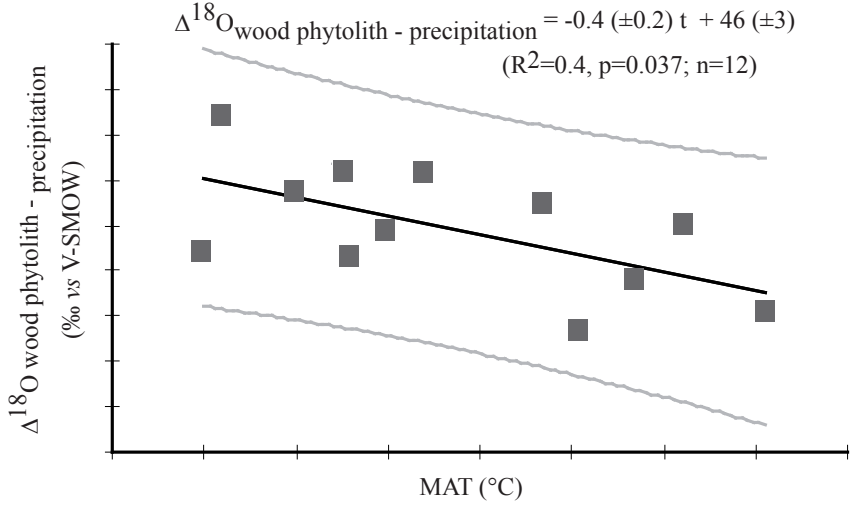

Fig. 5. Empirical relationship between $\Delta^{18}O_{wood\ phytolith-precipitation}$ value and mean annual atmospheric temperature (MAT) obtained for the three windward transects. Grey lines: limits of the 95 % confidence interval.

CPD
7, 1693–1735, 2011

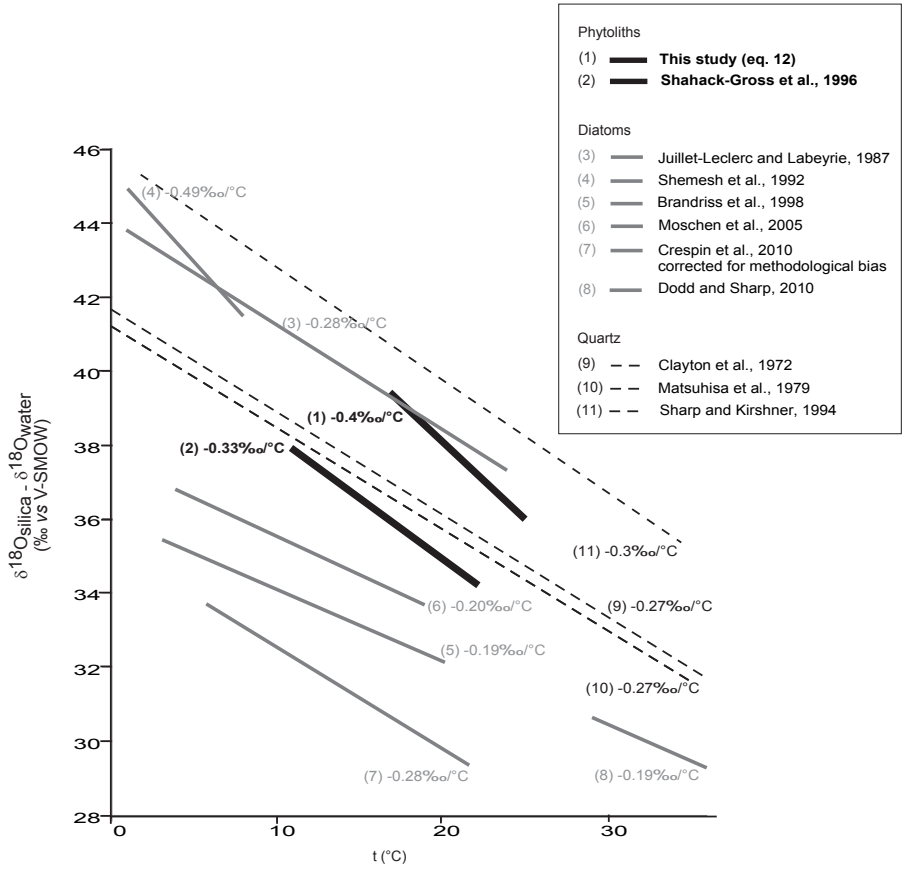

Fig. 6. Comparison of the thermo-dependant relationships expressed as 1000 lnα [$\delta^{18}O_{silica}$-$\delta^{18}O_{water}$] (‰ vs. VSMOW) = a t(°C) + b obtained for phytolith-water, diatom-water and quartz-water couples.

CPD
7, 1693–1735, 2011